ACS APPLIED MATERIALS & INTERFACES

Research Article

www.acsami.org

Ferromagnetic Sorbents Based on Nickel Nanowires for Efficient Uptake of Mercury from Water

Paula C. Pinheiro,[†] Daniela S. Tavares,[†] Ana L. Daniel-da-Silva,[†] Cláudia B. Lopes,[†] Eduarda Pereira,[†] João P. Araújo,[‡] Célia T. Sousa,[‡] and Tito Trindade*[,†]

[†]Department of Chemistry, CICECO and CESAM, Aveiro Institute of Nanotechnology, University of Aveiro, 3810-193 Aveiro, Portugal

[‡]IFIMUP and IN, Department of Physics, University of Porto, 4169-007 Porto, Portugal

ABSTRACT: This work reports the preparation of ferromagnetic nickel nanowires (NiNW) coated with dithiocarbamate-functionalized siliceous shells and its application for the uptake of aqueous Hg(II) ions by magnetic separation. NiNW with an average diameter and length of 35 nm and 5 μm, respectively, were firstly prepared by Ni electrodeposition in an anodic aluminum oxide template. The NiNW surfaces were then coated with siliceous shells containing dithiocarbamate groups via a one-step procedure consisting in the alkaline hydrolytic co-condensation of tetraethoxysilane (TEOS) and a siloxydithiocarbamate precursor (SiDTC). A small amount of these new nanoadsorbents (2.5 mg·L^{-1}) removed 99.8% of mercury ions from aqueous solutions with concentration 50 μg·L^{-1} and in less than 24 h of contact time. This outstanding removal ability is attributed to the high affinity of the sulfur donor ligands to Hg(II) species combined with the high surface area-to-volume ratio of the NiNW.

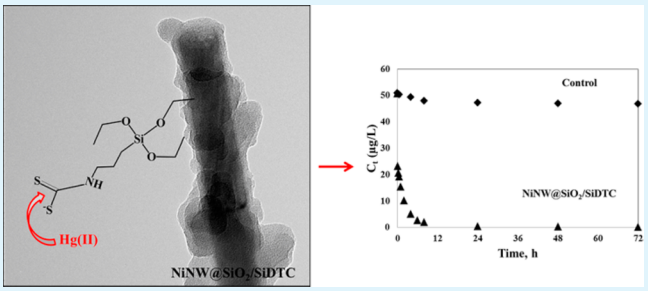

KEYWORDS: *nickel nanowires, ferromagnetic, mercury, dithiocarbamate, water quality monitoring*

INTRODUCTION

Water contamination by toxic metal ions such as mercury (Hg) is an eco-toxicological hazard of major interest that has raised the attention of the scientific community. Mercury and its compounds are highly toxic even in traces amounts.[1] Due to high toxicity to aquatic biota and humans, mercury is regarded as one of the priority hazardous substances by the European Union (EU) and according to the Water Framework Directive, all EU Member States must implement measures to progressively reduce its emissions, discharges, and losses.[2]

The unprecedented progress on methods of synthesis of nanomaterials has provided opportunities for the fabrication of nanostructured materials with tailored and improved properties desirable for water remediation and reuse, either by photocatalytic degradation, membrane filtration, or adsorption.[3−5] For example, nanosorbents offer significant improvement of the adsorption capacity over conventional adsorbents due to the high specific surface area, tunable pore size, and short intraparticle diffusion distance. Furthermore, the surface of many nanomaterials can be chemically modified to target specific pollutants, achieving high selectivity. In this context, several nanomaterials have been investigated as nanoadsorbents for the removal of Hg(II) species and other heavy-metal ions contaminants from water; examples of such type of sorbents include carbon-based nanomaterials[6] and polymer nanocomposites.[7]

Recently, a distinct approach for the removal of water contaminants have been developed, involving the use of magnetic nanoparticles.[8−10] Magnetic nanosorbents appear attractive because they can be easily separated from water under an external magnetic field. Iron oxides, namely magnetite (Fe_3O_4) and maghemite (γ-Fe_2O_3) are by far the materials most commonly used for preparing magnetic nanosorbents due to high surface area-to-volume ratio, good magnetic features, and ability for surface functionalization, associated with the relatively low cost and low toxicity.[8−11] Our interest in this field, prompted us to the development of magnetite particles coated with silica shells modified with dithiocarbamate groups.[12,13] These sorbents are highly effective in the decontamination of synthetic and natural waters containing realistic Hg(II) concentrations (50 μg·L^{-1}), by applying a relatively weak external magnetic field.[12−15] Even in more complex matrices, such as spiked surface-river water, these particles showed very good performance and it was possible to achieve Hg(II) levels below the guideline values established by the EU Water Framework directive.[14]

Nickel nanowires are high aspect ratio ferromagnetic particles with submicrometer diameters (8-500 nm) and lengths in the range from few nanometers to several micrometers. NiNW carry a permanent magnetic moment, and hence, they are readily oriented and manipulated in response to magnetic fields. In fact, NiNW have received considerable attention in cell manipulation,[16−20] micro-rheology,[21,22] and microfluidics.[23,24]

Received: February 21, 2014
Accepted: May 6, 2014
Published: May 6, 2014

   dx.doi.org/10.1021/am5010865 | ACS Appl. Mater. Interfaces 2014, 6, 8274−8280

For example, in specific applications such as cell separation, it was demonstrated that NiNW outperform magnetic spheroid beads of identical volume due to the higher magnetic moment of the nanowires compared to the beads.[18] In addition, NiNW have been exploited in analytical chemistry, such as amperometric sensors for the detection of glucose,[24−26] sucrose,[26] and methanol.[25] Despite being easily manipulated through the application of an external magnetic, NiNW remain to be exploited in water purification and monitoring technologies. Although NiNW pose some concerns related to their potential toxicity, they offer an alternative in specific contexts of application such as in laboratorial monitoring and analysis of water quality.

The present paper describes the first attempt to explore functionalized NiNW as nanosorbents for the removal of aqueous heavy metal ions, such as Hg(II). Therefore, ferromagnetic nickel nanowires have been coated with a siliceous shell containing dithiocarbamate groups in order to confer strong affinity to such ionic species and also to limit adventitious processes of lixiviation of the Ni particles. The resulting coated NiNW have shown efficient uptake of mercury from water, upon magnetic separation, thus demonstrating their potential for metal uptake and water quality monitoring.

EXPERIMENTAL PROCEDURES

Materials. High purity (>99.97 %) aluminum foils 250 μm thick were obtained from Alfa Aesar. Oxalic acid ($H_2C_2O_4$, ≥99 %), boric acid (H_3BO_3, ≥99.5 %), nickel(II) sulfate hexahydrate ($NiSO_4{\cdot}6H_2O$, 99 %), nickel(II) chloride hexahydrate ($NiCl_2{\cdot}6H_2O$, 99.9 %), phosphoric acid (H_3PO_4, 85%), chromium oxide (CrO_3, ≥99 %), tetraethyl orthosilicate ($Si(OC_2H_5)_4$:TEOS, >99%) and 3-aminopropyltriethoxysilane ($H_2N(CH_2)_3Si(OC_2H_5)_3$, APTES, >99%) were purchased from Sigma-Aldrich. Carbon disulfide (CS_2, >99%) and ethanol (CH_3CH_2OH, >99%) were obtained from Panreac. Sodium hydroxide (NaOH, >98%) was purchased from Pronolab and ammonia solution (NH_4OH, 25%) was obtained from Riedel-de-Haen. The certified standard stock solution of $Hg(NO_3)_2$ (998 ± 2 mg·L^{-1}) was purchased from Merck. All chemicals were used as received and all aqueous solutions were freshly prepared using ultrapure water (18.2 mΩ·cm^{-1}).

Synthesis of Siloxydithiocarbamate Precursor (SiDTC). The siloxydithiocarbamate compound (SiDTC) was obtained by conversion of APTES into the corresponding dithiocarbamate, by reaction with CS_2 in alkaline medium using sodium ethoxide as base.[13] Sodium ethoxide was obtained by reacting sodium hydroxide (0.2 g) in dry ethanol (25 mL) for 6 h and over a nitrogen atmosphere. The mixture was cooled to 273 K and then carbon disulfide (0.30 mL) and APTES (1.17 mL) have been added dropwise. After stirring at 273 K for 30 min, the mixture was heated at 313 K and left under vigorous stirring for 24 h. After cooling to room temperature, the volatiles were evaporated under a dynamic vacuum.

Synthesis of SiO_2/SiDTC Coated NiNW. Ni nanowires were fabricated by electrodeposition method, using anodized aluminum oxide (AAO) membrane.[19] The synthesis of SiO_2/SiDTC coated nickel nanowires (NiNW@SiO_2/SiDTC) was performed by a one-step procedure that included the alkaline hydrolysis of TEOS in the presence of the precursor SiDTC. Hence, a dispersion of NiNW (5 mg) in ethanol (3.8 mL) was prepared and left immersed in an ice bath, over 4 min under sonication (horn Sonics, Vibracell). Consecutively, ammonia solution (0.3 mL) and a mixture of SiDTC and TEOS (3.7 mg and 8.3 μL, respectively) were added, and the resulting suspension was left in an ice bath for 30 min, under sonication. Finally, the nanowires were collected using a NdFeB magnet and washed thoroughly with ethanol.

Silica coating of NiNW was performed similarly via the alkaline hydrolysis of TEOS as the only Si alkoxide precursor present.

Uptake of Mercury Ions from Water. The ability of NiNW, NiNW@SiO_2, and NiNW@SiO_2/SiDTC to uptake Hg(II) was evaluated by contacting the particles with a known concentration (50μg·L^{-1}) of an aqueous solution of Hg(II) for variable periods of time. The sorption experiments were carried out in a 500 mL glass batch reactor at 295 ± 1 K, under mechanical stirring using a glass rod. The pH of all working Hg(II) solutions was adjusted to 7 using 0.1 mol·L^{-1} aqueous NaOH. An amount (2.5 mg·L^{-1}) of the sorbent (NiNW, NiNW@SiO_2, or NiNW@SiO_2/SiDTC) was added to the Hg(II) aqueous solutions. For each experiment, the Hg(II) solution was stirred continuously, and aliquots were withdrawn at increasing contact times (t). A control experiment without sorbent was carried out in parallel. Hg(II) was quantified by atomic fluorescence spectroscopy, on a flow-injection cold vapor atomic fluorescence spectrometer (hydride/vapor generator PS Analytical Model 10.003, coupled to a PS Analytical Model 10.023 Merlin atomic fluorescence spectrometer), which allows Hg(II) detection at very low levels (2 ng·L^{-1}). All glassware used in the sorption studies were acid washed (nitric acid 25%, 12 h) and then rinsed by ultra-pure water.

The amount of Hg(II) sorbed at each time (q_{Hg}) was calculated by material balance according to $q_{Hg} = (C_{Hg,0} - C_{Hg,t})Vm^{-1}$, where $C_{Hg,0}$ is the initial Hg(II) concentration in solution and $C_{Hg,t}$ is the Hg(II) concentration in solution at time t (both in microgram per liter), V is the volume of solution (in liter), and m is the mass of sorbent (in gram). The experimental data were modeled using three, of the most used kinetic models in this field, the pseudo-first- and the pseudo-second-order models[27,28] and the Elovich model,[29] expressed respectively by the following equations:

$$q_{Hg} = q_{Hg,e}(1 - e^{-k_1 t})$$

$$q_{Hg} = \frac{q^2_{Hg,e} k_2 t}{1 - q_{Hg,e} k_2 t}$$

$$q_{Hg} = \frac{1}{\beta}\ln(1 + \alpha\beta t)$$

where $q_{Hg,e}$ (in microgram per gram) is the amount of Hg(II) sorbed per gram of sorbent, at equilibrium, k_1 (in per hours), and k_2 (in gram per microgram per hour) are respectively the kinetic constants of pseudo-first- and pseudo-second-order, α (in microgram per gram per hour) is the initial sorption rate and β (in gram per microgram) is the desorption constant.

The kinetic parameters were obtained by nonlinear regression analysis using the GraphPad Prism 5 program (trial version). This program uses the least-squares as fitting method and the method of Marquardt and Levenberg, blending the methods of linear descent and Gauss−Newton for adjusting the variables. The goodness of the fits to the experimental data was evaluated by the coeficient of regression (R^2) and the standard deviation of residues ($S_{x/y}$).

Characterization. Fourier transform infrared (FTIR) spectra were recorded using a spectrometer Bruker Optics Tensor 27 coupled to a horizontal attenuated total reflectance (ATR) cell, using 256 scans at a resolution of 4 cm^{-1}. SEM was performed using a scanning electron microscope Hitachi S4100 operating at an accelerating voltage of 25 kV. For SEM analysis, aliquots of diluted suspensions containing the nanowires were allowed to air dry on glass slides and then were coated with evaporated carbon. Transmission electron microscopy (TEM) images were obtained by using a JEOL 2200FS microscope. Samples for TEM analysis were prepared by evaporating diluted suspensions of the nanowires on a copper grid coated with amorphous carbon film. The powder X-ray diffraction patterns were recorded using an X-ray diffractometer Philips X'Pert equipped with a Cu Kα monochromatic radiation source. Elemental analysis of carbon, nitrogen, hydrogen, and sulfur was performed using an Eager 300 instrument and the elemental analysis of Si was performed by inductively coupled plasma (ICP) spectroscopy using a Jobin-Yvon JY70 Plus spectrometer. All concentration values of mercury in the water samples were obtained by using an atomic fluorescence spectrometer (hydride/vapor generator PS analytical model 10.003, coupled to a PS analytical model 10.023 Merlin atomic fluorescence spectrometer) and using $SnCl_2$ (10% m/v) as a reducing agent. The Hg(II) concentration was quantified through a calibration curve of five

standards (0.0 to 0.5 mg·L^{-1}) prepared in a HNO_3 solution (2% v/v), by dilution from the certified standard stock solution of mercury nitrate (998 ± 2 mg·L^{-1}). The concentration of Ni in the tested solutions, as consequence of adventitious dissolution of the sorbents, was quantified by inductively coupled plasma spectroscopy (ICP-OES), using a Jobin-Yvon JY70 Plus Spectrometer. The magnetization measurements were performed using a commercial superconducting quantum interface device (SQUID; Quantum Design), operating at room temperature, with an applied magnetic field up 2 T, with adjustable sample position parallel/perpendicular to the magnetic field. The NiNW were firstly measured still inside the AAO membrane with the magnetic field parallel and perpendicular to the wires axis. Then, the alumina membrane was removed using NaOH 1M. The powders were then thoroughly washed with water and dried under a N_2 stream. Finally, the powders were placed in a diamagnetic sample holder where the measurements were performed.

RESULTS AND DISCUSSION

Synthesis and Characterization of Materials. The NiNW used in this research were produced by a template-assisted method, using Ni electrodeposition in AAO templates. The powders obtained were characterized by XRD (data not shown) confirming unequivocally the presence of face-centered cubic Ni due to the presence of three main reflections corresponding to the (111), (220), and (200) planes of fcc Ni, with the relative higher intensity of the (111) reflection at 2θ = 45° ascribed to the anisotropic growth of these nanostructures.[19] Prior to the NiNW surface modification, a siloxydithiocarbamate precursor (SiDTC) was synthesized by conversion of APTES into the corresponding dithiocarbamate in alkaline medium following a procedure described previously.[13] In the present research, this compound was investigated as a precursor that together with TEOS reacts by hydrolytic and condensation reactions in ethanol, in order to generate hybrid siliceous shells functionalized with dithiocarbamate groups at the surface of NiNW. This chemical surface modification of NiNW with hybrid siliceous shells was carried out in order to upgrade the native NiNW, aiming at the removal of mercury ions from aqueous solutions by magnetic separation.

The sorbent materials have been characterized before contacting with the Hg(II) aqueous solutions. Thus, Figure 1 shows the results obtained by microscopy analysis performed on the original NiNW (Figure 1-top) and the modified samples after surface coating via alkaline hydrolysis of TEOS in the presence of SiDTC (Figure 1-bottom). For comparative purposes, NiNW with amorphous SiO_2 shells have also been prepared (Figure 1-middle). The NiNW present a diameter and length of about 35 nm and 5 μm, corresponding to the AAO pore diameter and template thickness, respectively. The SEM and TEM images clearly show an amorphous coating of about 18 nm thickness for both NiNW samples treated with TEOS and TEOS/SiDTC, though distinct in the morphological characteristics. While the SiO_2 coating appeared as uniform shells over the NiNW, the hydrolysis of TEOS/SiDTC mixtures resulted into coatings presenting discrete bumps over the film coating. The chemical analysis (Table 1) together with the FTIR (Figure 2) spectrum of the latter confirmed the presence of a siliceous network enriched in sulfur, as reported previously for the surface modification of magnetite particles.[13]

A typical hysteresis loop for NiNW with high aspect ratio inside the AAO template (NiNW diameter =35 nm, inter-wire distance = 105 nm, and NiNW length = 5 μm) is shown in Figure 3 (left). The hysteresis loops measured at room temperature

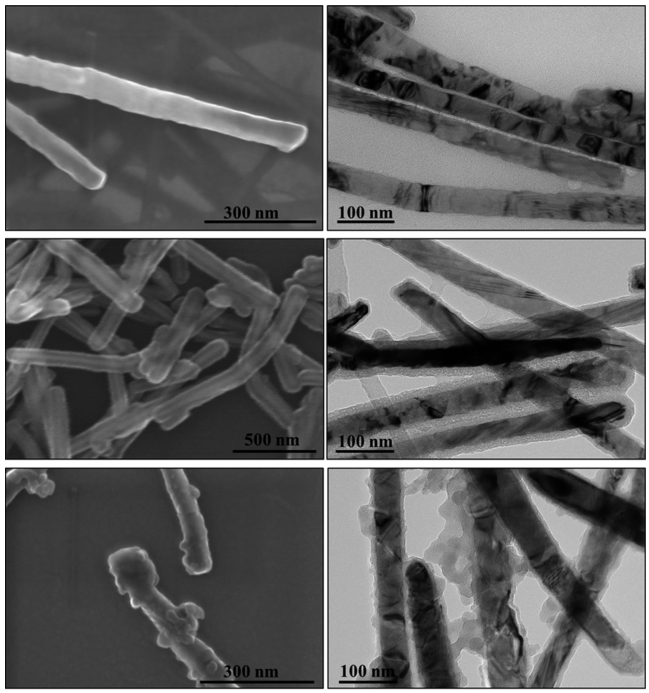

Figure 1. SEM (left panel) and TEM (right panel) images of Ni nanowires prepared by electrodeposition in AAO template. Top: original NiNW. Middle: NiNW coated with amorphous silica. Bottom: NiNW coated with silica shells containing dithiocarbamate groups.

Table 1. Elemental Analysis of as Prepared NiNW@SiO_2/SiDTC Sorbents

sample	C (%)	H (%)	N (%)	S (%)
NiNW	0.42	0.40	0.00	0.00
NiNW@SiO_2/SiDTC	4.00	1.45	1.26	1.86

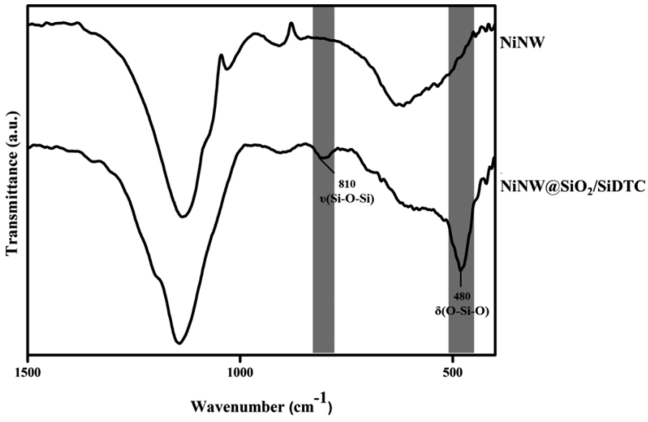

Figure 2. ATR-FTIR spectra of NiNW and NiNW@SiO_2/SiDTC samples.

with the applied field parallel and perpendicular to the wires axes exhibit an anisotropic behavior with the parallel loop showing larger values of remanence and coercivity. This corresponds to an easy axis along the longitudinal NiNW direction with saturation field (H_{Sat}) of 2 kOe and (NiNW with aspect ratio 30:1) of 1000 Oe and a hard axis along the NiNW axial direction (H_{Sat} = 13 kOe; H_c = 120 Oe). Due to the shape effect (coercive field (H_c)), and the low template porosity (10%), the shape anisotropy overcomes

dx.doi.org/10.1021/am5010865 | ACS Appl. Mater. Interfaces 2014, 6, 8274−8280

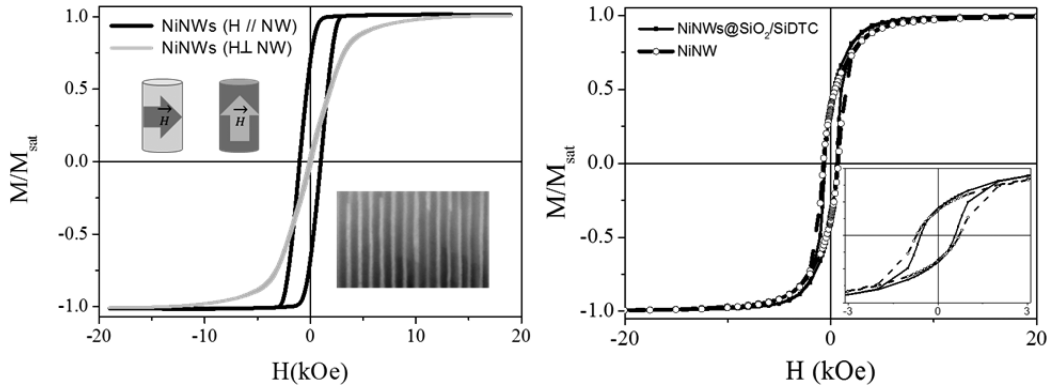

Figure 3. Left panel: magnetization behavior of NiNW inside the AAO membrane, transverse (gray line), and parallel (black line) to NWs long axis; SEM image of the membrane with NiNW in inset. Right panel: room temperature M(H) curve for NiNW (dashed line) and NiNW@SiO_2/SiDTC (solid line) powders.

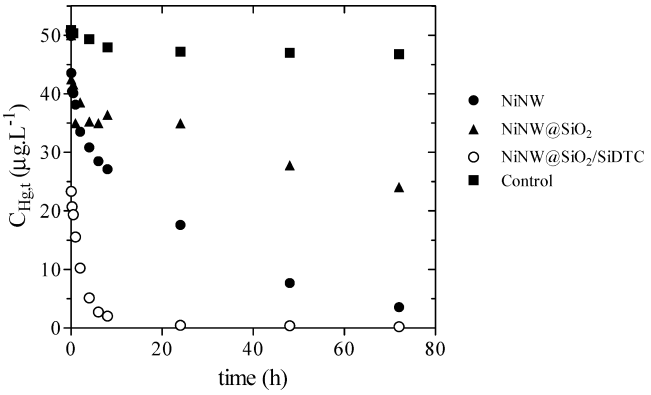

Figure 4. Concentration of Hg(II) in aqueous solutions as a function of contact time with distinct Ni based sorbents.

all the other contributions for the total magnetic anisotropy and the NiNW should be preferentially magnetized along the wire longitudinal axis, as observed.[30−32] Figure 3 (right− solid line) shows typical hysteresis loop for a ferromagnetic NiNW powder after AAO membrane removal. Out of the membrane, the random NiNW present a H_c = 700 Oe, H_{Sat} = 15 kOe, and M_{sat} = 49.5 emu/g.[33] In this case, a behavior of an isotropic system is observed where the magnetic anisotropy is governed mainly by the dipolar interactions.[32,34] The functionalized NiNW@SiO_2/SiDTC sample presents a similar hysteresis loop of the powder NiNW, as shown in Figure 3 (right−dashed line) with H_c = 570 Oe. This decrease of the NiNW@SiO_2/SiDTC coercivity can be attributed to the NiNW functionalization, which increases the inter-wire distance and therefore the wires interactions.

Removal of Aqueous Hg(II) Using Magnetic Sorbents. The potential of ferromagnetic NiNW for environmental applications will increase by promoting a functionalized surface adequate for pollutants uptake, such as heavy metal ions. In fact, here the surfaces of the NiNW have been designed aiming strong affinity for Hg(II), which is well known as a highly polarizable Lewis acid (*soft acid*).[35] In line with the hard-soft/acid−base formalism proposed by Pearson,[35] there is strong affinity of S donors towards mercury. In this research, surfaces enriched in dithiocarbamate ligands (*soft base*) were used as coatings for the NiNW and the resulting materials were investigated for Hg(II) uptake from water samples. Figure 4 shows the curves obtained from such experiments in which the NiNW, NiNW@SiO_2, and NiNW@SiO_2/SiDTC samples have been used. In Figure 4, the *y*-axis represents the amount of Hg(II) ($C_{Hg,t}$) remaining in solution after contact time *t* with the magnetic sorbents. This Figure shows a decrease of $C_{Hg,t}$ along time that approaches an equilibrium concentration for all the magnetic samples analyzed. Note that the original NiNW also shows sorbent capacity for mercury ions, which can be explained by the presence of a native oxide layer at the metal surface.[20] Also, SiO_2 surfaces are known to act themselves as sorbents for several cationic species, which explain the results observed for the NiNW@SiO_2. Nevertheless the sorbent efficiency clearly increased for the NiNW@SiO_2/SiDTC sample, which we interpret as a result of the presence of the dithiocarbamate moieties at the SiO_2 network. Under the experimental conditions used in this work, 2.5 mg·L^{-1} of this sorbent could reduce the initial concentration ($C_{Hg,0}$) of Hg(II) from 50 μg·L^{-1} to a residual concentration ($C_{Hg,>8h}$) lower than 1 μg·L^{-1} (guideline value for drinking water quality[36]). It should be noted that for this material the removal percentage of Hg(II) was higher than 99.8%. Also note that at pH 7 and for initial Hg(II) concentrations less than 120 mg·L^{-1}, it has been reported that the formation of $Hg(OH)_2$ precipitates does not occur.[37]

Some relevant differences were observed on the Hg(II) sorption kinetics for the materials under analysis. Clearly, the sorption rate of Hg(II) onto NiNW@SiO_2/SiDTC materials was higher than onto sorbents without dithiocarbamate moieties (Figure 4), which allowed the concentration of Hg(II) to equilibrate in less than 24 h for the former case. In fact, an estimate of the initial sorption rate (t = 0) for all systems shows that for the NiNW@SiO_2/SiDTC sample the initial rate is 480 μg·g^{-1}·h^{-1}, while for the NiNW and NiNW@SiO_2 samples the respective values are 105 and 130 μg·g^{-1}·h^{-1}; the initial sorption rates were estimated from the first derivative of the $C_{Hg} = f(t)$ curve at t = 0. The time evolution of the experimental and modelled data of Hg(II) content in the sorbents (q_{Hg}) are shown in Figure 5.

For the Hg(II):NiNW and Hg(II):NiNW@SiO_2/SiDTC systems, the results showed a good agreement between data and the fittings accomplished by the Elovich model (respectively, R^2=0.96, $S_{y/x}$ = 1.20 and R^2=0.99, $S_{y/x}$ = 0.77), followed by the pseudo-second-order model (respectively, R^2=0.90, $S_{y/x}$ = 1.93 and R^2=0.91, $S_{y/x}$ = 1.93). Furthermore, the kinetic constants k_2 and α, confirmed that Hg(II) sorption onto NiNW@SiO_2/SiDTC was faster than when NiNW was used (Table 2). The $q_{Hg,e}$ values estimated by the pseudo-second-order model (Table 2) match the experimental data, showing a relative standard error that ranges from 3.6 to 8.5%. For the Hg(II):NiNW@SiO_2 system only the Elovich

dx.doi.org/10.1021/am5010865 | ACS Appl. Mater. Interfaces 2014, 6, 8274−8280

Table 2. Kinetic Parameters Estimated by the Pseudo-first- and Pseudo-second-order and Elovich Models for the Hg^{II}:NiNW, Hg^{II}:NiNW@SiO_2, and Hg^{II}:NiNW@SiO_2/SiDTC Systems, and the Experimental $q_{Hg,e}$ Values Obtained for Each System*

	experimental	pseudo-first-order		pseudo-second-order		Elovich	
system	$q_{Hg,e}$ ($\mu g \cdot g^{-1}$)	$q_{Hg,e}$ ($\mu g \cdot g^{-1}$)	k_1 (h^{-1})	$q_{Hg,e}$ ($\mu g \cdot g^{-1}$)	k_2 ($g \cdot \mu g^{-1} \cdot h^{-1}$)	α ($\mu g \cdot g^{-1} \cdot h^{-1}$)	β ($g \cdot \mu g^{-1}$)
Hg^{II}:NiNW	18.7	16.3 (1.45)	0.15 (0.04)	18.5 (1.60)	0.011 (0.004)	10.8 (3.3)	0.32 (0.03)
Hg^{II}:NiNW@SiO_2	10.5	7.08 (0.80)	1.90 (1.10)	7.85 (0.85)	0.214 (0.146)	88.7 (71.6)	0.979 (0.150)
Hg^{II}:NiNW@SiO_2/SiDTC	19.9	17.0 (1.08)	6.85 (2.64)	18.2 (0.90)	0.495 (0.187)	4492 (2665)	0.53 (0.04)

*The standard errors for each parameter are shown in parentheses.

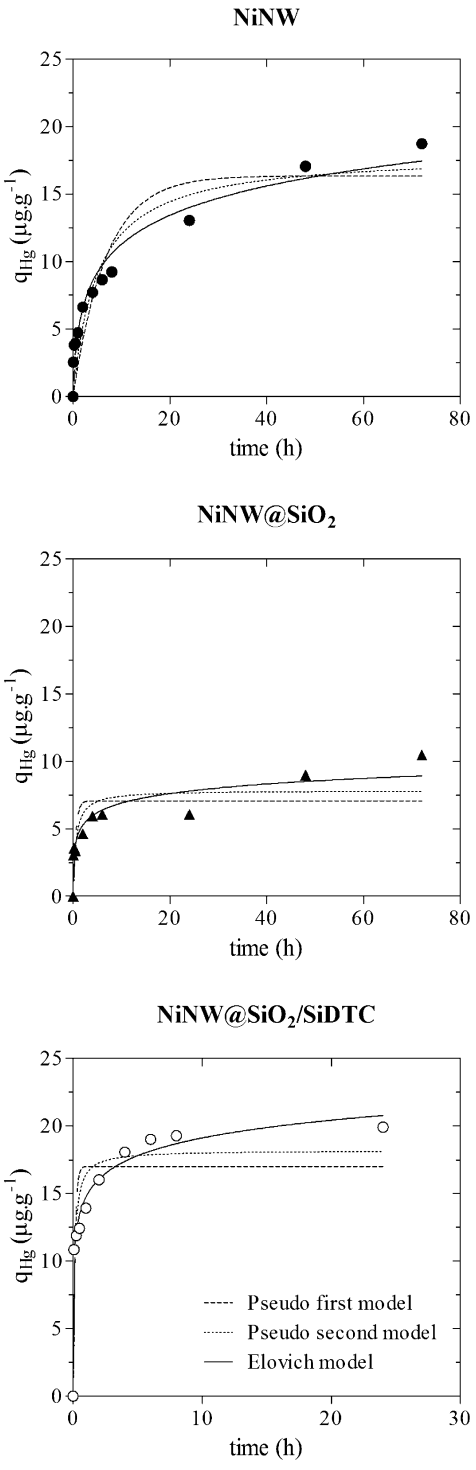

Figure 5. Experimental and modeling results for the amount of Hg(II) in the sorbents NiNW, NiNW@SiO_2, and NiNW@SiO_2/SiDTC, in function of time.

model was able to fit the experimental data accurately (R^2=0.91, $S_{y/x}$ = 0.95).

Although the study of eventual lixiviation of the sorbents for different removal conditions was out of the scope of this research, we decided to assess preliminary this effect on the final characteristics of the particles. Hence, the NiNW@SiO_2/SiDTC samples that have contacted with water samples were collected magnetically for further microscopic analysis. Figure 6

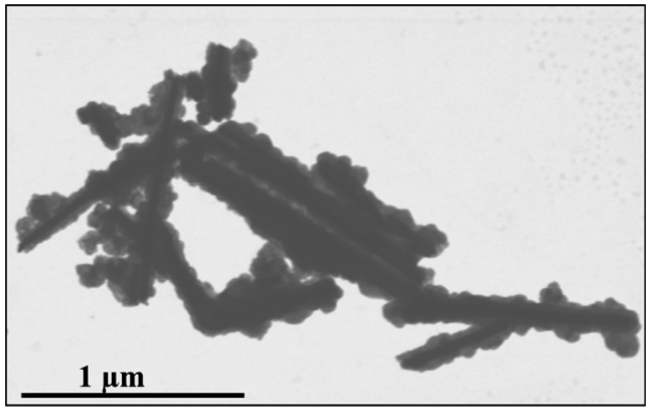

Figure 6. STEM image (transmission mode) of NiNW@SiO_2/SiDTC after 72 h contact with a Hg(II) aqueous solution.

shows no significant morphological changes on the surface modified nanowires after contact with the Hg(II) aqueous solutions, as compared to the original sample (Figure 1). Also, the solutions have been analyzed by ICP for the amount of Ni present after a contact time of 24 h with the sorbent; at this time, 99.8% of Hg(II) was removed when using the NiNW@SiO_2/SiDTC sample. In this case, a maximum value of 57 $\mu g \cdot L^{-1}$ was registered for the nickel concentration while for the uncoated NiNW the amount of nickel in water varied along the time of the experiment but reached a maximum value of 347 $\mu g \cdot L^{-1}$. Although these results suggest that the hybrid siliceous shells protect to some extent the coated NiNW against dissolution, further studies are required to assess the robustness of these materials in several working conditions.

CONCLUSIONS

In conclusion, this research described the first use of NiNW for the magnetic assisted removal of water pollutants, such as aqueous Hg(II). The Ni nanostructures have been coated with hybrid shells composed of amorphous silica and dithiocarbamate moieties, which accounts for their high efficiency for aqueous Hg(II) uptake. Indeed, the Hg removal percentage (99.8 %) found for these new sorbents is comparable to that reported previously for magnetite nanoparticles functionalized with dithiocarbamate groups[13] and superior to that found for ETS-4 titanosilicate sorbents (96.4%),[38] using similar removal

conditions. This type of architecture for the surface modified NiNW not only allowed efficient metal uptake but can also be further exploited in laboratorial monitoring for water quality analysis, namely by adapting the nanowires as platforms for environmental sensors. In this regards, the coupling of these ferromagnetic nanostructures to optical responsive materials is in perspective.

AUTHOR INFORMATION

Corresponding Author

*Email: tito@ua.pt. Fax: +351 234 370 084. Tel: +351 234 370 726.

Author Contributions

The manuscript was written through contributions of all authors. All authors have given approval to the final version of the manuscript.

Notes

The authors declare no competing financial interest.

ACKNOWLEDGMENTS

This work was financed by national funding from FCT (Fundação para a Ciência e a Tecnologia) through the project PTDC/CTM-NAN/120668/2010, by FEDER through program COMPETE, and through FCT/FEDER in the frame of projects Pest-C/CTM/LA0011/2013 and Pest-C/MAR/LA0017/2013. P. C. Pinheiro thanks FCT for the grant SFRH/BD/96731/2013. C. T. Sousa thanks FCT for the grant SFRH/BPD/82010/2011. We thank the RNME (National Electronic Microscopy Network) for microscopy facilities.

ABBREVIATIONS

NiNW = nickel nanowires
TEOS = tetraethoxysilane
SiDTC = siloxydithiocarbamate precursor
EU = European Union
APTES = 3-aminopropyl triethoxysilane
AAO = anodized aluminum oxide
NiNW@SiO_2/SiDTC = SiO_2/SiDTC coated nickel nanowires
NiNW@SiO_2 = SiO_2 coated nickel nanowires
FTIR = Fourier transform infrared
TEM = transmission electron microscopy
SEM = scanning electron microscopy
ICP = inductively coupled plasma spectroscopy
XRD = powder X-ray diffraction

REFERENCES

(1) Nordberg, G. F.; Fowler, B. A.; Nordberg, M.; Friberg, L. T. *Handbook on the Toxicology of Metals*, 3rd ed; Academic Press: San Diego, 2007.

(2) Council on Establishing a Framework for Community Action in the Field of Water Policy. *Official Journal of the European Communities*; **2000**.

(3) Khin, M. M.; Nair, A. S.; Babu, V. J.; Murugan, R.; Ramakrishna, S. A Review on Nanomaterials for Environmental Remediation. *Energy Environ. Sci.* **2012**, *5*, 8075−8109.

(4) Qu, X.; Brame, J.; Li, Q.; Alvarez, P. J. J. Nanotechnology for a Safe and Sustainable Water Supply: Enabling Integrated Water. *Acc. Chem. Res.* **2013**, *46*, 834−843.

(5) Kurniawan, T. A.; Sillanpää, M. E. T.; Sillanpää, M. Nanoadsorbents for Remediation of Aquatic Environment: Local and Practical Solutions for Global Water Pollution Problems. *Crit. Rev. Environ. Sci. Technol.* **2012**, *42*, 1233−1295.

(6) Mubarak, N. M.; Sahu, J. N.; Abdullah, E. C.; Jayakumar, N. S. Removal of Heavy Metals from Wastewater using Carbon Nanotubes. *Sep. Purif. Rev.* **2014**, *43*, 311−338.

(7) Zhao, X.; Lv, L.; Pan, B.; Zhang, W.; Zhang, S.; Zhang, Q. Polymer-Supported Nanocomposites for Environmental Application: A Review. *Chem. Eng. J.* **2011**, *170*, 381−394.

(8) Tang, S. C. N.; Lo, I. M. C. Magnetic Nanoparticles: Essential Factors for Sustainable Environmental Applications. *Water Res.* **2013**, *47*, 2613−2632.

(9) Ambashta, R. D.; Sillanpää, M. Water Purification using Magnetic Assistance: A Review. *J. Hazard. Mater.* **2010**, *180*, 38−49.

(10) Xu, P.; Zeng, G. M.; Huang, D. L.; Feng, C. L.; Hu, S.; Zhao, M. H.; Lai, C.; Wei, Z.; Huang, C.; Xie, G. X.; Liu, Z. F. Use of Iron Oxide Nanomaterials in Wastewater Treatmente: A Review. *Sci. Total Environ.* **2012**, *424*, 1−10.

(11) Daniel-da-Silva, A. L.; Carvalho, R. S.; Trindade, T. Magnetic Hydrogel Nanocomposites and Composite Nanoparticles—A Review of Recent Patented Works. *Recent Pat. Nanotechnol.* **2013**, *7*, 153−166.

(12) Girginova, P. I.; Daniel-da-Silva, A. L.; Lopes, C. B.; Figueira, P.; Otero, M.; Amaral, V. S.; Pereira, E.; Trindade, T. Silica Coated Magnetite Particles for Magnetic Removal of Hg^{2+} from Water. *J. Colloid Interface Sci.* **2010**, *345*, 234−240.

(13) Tavares, D. S.; Daniel-da-Silva, A. L.; Lopes, C. B.; Silva, N. J. O.; Amaral, V. S.; Rocha, J.; Pereira, E.; Trindade, T. Efficient Sorbents Based on Magnetite Coated with Siliceous Hybrid Shells for Removal of Mercury Ions. *J. Mater. Chem. A* **2013**, *1*, 8134−8143.

(14) Lopes, C. B.; Figueira, P.; Tavares, D. S.; Lin, Z.; Daniel-da-Silva, A. L.; Duarte, A. C.; Rocha, J.; Trindade, T.; Pereira, E. Core−Shell Magnetite−Silica Dithiocarbamate-derivatized Particles Achieve the Water Framework Directive Quality Criteria for Mercury in Surface Waters. *Environ. Sci. Pollut. Res.* **2013**, *20*, 5963−5974.

(15) Figueira, P.; Lopes, C. B.; Daniel-da-Silva, A. L.; Pereira, E.; Duarte, A. C.; Trindade, T. Removal of Mercury (II) by Dithiocarbamate Surface Functionalized Magnetite Particles: Application to Synthetic and Natural Spiked Waters. *Water Res.* **2011**, *45*, 5773−5784.

(16) Hultgren, A.; Tanase, M.; Felton, E. J.; Bhadriraju, K.; Salem, A. K.; Chen, C. S.; Reich, D. H. Optimization of Yield in Magnetic Cell Separations using Nickel Nanowires of Different Lengths. *Biotechnol. Prog.* **2005**, *21*, 509−515.

(17) Johansson, F.; Jonsson, M.; Alm, K.; Kanje, M. Cell Guidance by Magnetic Nanowires. *Exp. Cell Res.* **2010**, *316*, 688−694.

(18) Hultgren, A.; Tanase, M.; Chen, C. S.; Meyer, G. J.; Reich, D. H. Cell Manipulation Using Magnetic Nanowires. *J. Appl. Phys.* **2003**, *93*, 7554−7556.

(19) Pinheiro, P. C.; Sousa, C. T.; Araújo, J. P.; Guiomar, A. J.; Trindade, T. Functionalization of Nickel Nanowires with a Fluorophore Aiming at New Probes for Multimodal Bioanalysis. *J. Colloid Interface Sci.* **2013**, *410*, 21−26.

(20) Prina-Mello, A.; Diao, Z.; Coey, J. M. D. Internalization of Ferromagnetic Nanowires by Different Living Cells. *J. Nanobiotechnology* **2006**, *4*, 1−11.

(21) Cappallo, N.; Lapointe, C.; Reich, D. H.; Leheny, R. L. Nonlinear Microrheology of Wormlike Micelle Solutions using Ferromagnetic Nanowire Probes. *Phys. Rev. E: Stat., Nonlinear, Soft Matter Phys.* **2007**, *76*, 0315051−0315056.

(22) Tokarev, A.; Luzinov, I.; Owens, J. R.; Kornev, K. G. Magnetic Rotational Spectroscopy with Nanorods to Probe Time-dependent Rheology of Microdroplets. *Langmuir* **2012**, *28*, 10064−10071.

(23) Tanase, M.; Felton, E. J.; Gray, D. S.; Hultgren, A.; Chen, C. S.; Reich, D. H. Assembly of Multicellular Constructs and Microarrays of Cells using Magnetic Nanowires. *Lab Chip* **2005**, *5*, 598−605.

(24) Piccin, E.; Laocharoensuk, R.; Burdick, J.; Carrilho, E.; Wang, J. Adaptive Nanowires for Switchable Microchip Devices. *Anal. Chem.* **2007**, *79*, 4720−4723.

(25) Wang, J.; Scampicchio, M.; Laocharoensuk, R.; Valentini, F.; Gonzalez-García, O.; Burdick, J. Magnetic Tuning of the Electrochemical Reactivity through Controlled Surface Orientation of Catalytic Nanowires. *J. Am. Chem. Soc.* **2006**, *128*, 4562−4563.

(26) García, M.; Escarpa, A. Disposable Electrochemical Detectors based on Nickel Nanowires for Carbohydrate Sensing. *Biosens. Bioelectron.* **2011**, *26*, 2527−2533.
(27) Lagergren, S. K. About the Theory of So-called Adsorption of Soluble Substances. *K. Sven. Vetenskapsakad. Handl.* **1898**, *4*, 1−39.
(28) Ho, Y. S.; McKay, G. Pseudo-second Order Model for Sorption Processes. *Process Biochem.* **1999**, *34*, 451−465.
(29) Low, M. J. D. Kinetics of Chemisorption of Gases on Solids. *Chem. Rev.* **1960**, *60*, 267−312.
(30) Leitão, D. C.; Sousa, C. T.; Ventura, J.; Carpinteiro, F.; Amado, M.; Araújo, J. P.; Sousa, J. B. Influence of Surface Pre-treatment in the Room Temperature Fabrication of Nanoporous Alumina. *Phys. Status Solidi C* **2008**, *5*, 3488−3491.
(31) Vázquez, M.; Pirota, K.; Hernández-Vélez, M.; Prida, V. M.; Navas, D.; Sanz, R.; Batallan, F.; Velazquez, J. Magnetic Properties of Densely Packed Arrays of Ni Nanowires as a Function of their Diameter and Lattice Parameter. *J. Appl. Phys.* **2004**, *95*, 6642−6644.
(32) Encinas-Oropesa, A.; Demand, M.; Piraux, L.; Huynen, I.; Ebels, U. Dipolar Interactions in Arrays of Nickel Nanowires Studied by Ferromagnetic Resonance. *Phys. Rev. B* **2001**, *63*, 1044151−1044156.
(33) Proença, M. P.; Sousa, C. T.; Ventura, J.; Vazquez, M.; Araujo, J. P. Ni Growth Inside Ordered Arrays of Alumina Nanopores: Enhancing the Deposition Rate. *Electrochim. Acta* **2012**, *72*, 215−221.
(34) Nielsch, K.; Wehrspohn, R. B.; Barthela, J.; Kirschner, J.; Fischer, S.F.; Kronmuller, H.; Schweinböck, T.; Weiss, D.; Gosele, U. High Density Hexagonal Nickel Nanowire Array. *J. Magn. Magn. Mater.* **2002**, *249*, 234−240.
(35) Pearson, R. G. Acids and Bases. *Science* **1966**, *151*, 172−177.
(36) Council Directive 98/83/EC on the Quality of Water Intended for Human Consumption. *Official Journal of the European Communities*; **1998**.
(37) Zhang, F.-S.; Nriagu, J.O.; Itoh, H. Mercury Removal from Water using Activated Carbons Derived from Organic Sewage Sludge. *Water Res.* **2005**, *39*, 389−395.
(38) Lopes, C. B.; Otero, M.; Lin, Z.; Silva, C. M.; Rocha, J.; Pereira, E.; Duarte, A. C. Removal of Hg^{2+} Ions from Aqueous Solution by ETS-4 Microporous Titanosilicate—Kinetic and Equilibrium Studies. *Chem. Eng. J.* **2009**, *151*, 24−254.